Muehlematter, D., Larsson, R., & Cerutti, P. (1988) *Carcinogenesis 9*, 239–245.
Muller, W., & Zahn, R. (1976) *Mol. Cell. Biochem. 12*, 147–159.
Niedergang, C., Muricia, G., Ittel, M. A., Pouyet, J., & Mandel, P. (1985) *Eur. J. Biochem. 146*, 185–191.
Ohashi, Y., Ueda, K., Kawaichi, M., & Hayaishi, O. (1983) *Proc. Natl. Acad. Sci. U.S.A. 80*, 3604–3607.
Poirier, G., Murcia, G., Jongstra-Bilen, J., Niedergang, C., & Mandel, P. (1982) *Proc. Natl. Acad. Sci. U.S.A. 79*, 3423–3427.
Singh, N., Leduc, Y., Poirier, G., & Cerutti, P. (1985) *Carcinogenesis 6*, 1489–1494.
Teraoka, H., Sumikawa, T., & Isukaka, K. (1986) *J. Biol. Chem. 261*, 6888–6892.
Towbin, H., Staehelin, T., & Gordon, J. (1979) *Proc. Natl. Acad. Sci. U.S.A. 76*, 4350–4354.
Wang, J. (1981) Type I DNA topoisomerase. *Enzymes (3rd Ed.) 14*, 331–344.
Wang, J. (1987) *Biochim. Biophys. Acta 909*, 1–9.
Wesierska-Gadek & Sauermann, G. (1985) Modification of nuclear matrix proteins by ADP-ribosylation. *Eur. J. Biochem. 153*, 421–428.
Yang, L., Wold, M., Li, J., Kelly, T., & Liu, L. (1987) *Proc. Natl. Acad. Sci. U.S.A. 84*, 950–954.

Time-Resolved Fluorescence Spectroscopy of Human Adenosine Deaminase: Effects of Enzyme Inhibitors on Protein Conformation†

Anne V. Philips and Mary Sue Coleman*
Department of Biochemistry and Lucille P. Markey Cancer Center, University of Kentucky, Lexington, Kentucky 40536-0084
Karol Maskos and Mary D. Barkley*
Department of Chemistry, Louisiana State University, Baton Rouge, Louisiana 70803
Received August 16, 1988; Revised Manuscript Received October 25, 1988

ABSTRACT: Adenosine deaminase, a purine salvage enzyme essential for immune competence, was studied by time-resolved fluorescence spectroscopy. The heterogeneous emission from this four-tryptophan protein was separated into three lifetime components: τ_1 = 1 ns and τ_2 = 2.2 ns with an emission maximum at about 330 nm and τ_3 = 6.3 ns with emission maximum at about 340 nm. Solvent accessibility of the tryptophan emission was probed with polar and nonpolar fluorescence quenchers. Acrylamide, iodide, and trichloroethanol quenched emission from all three components. Acrylamide quenching caused a blue shift in the decay-associated spectrum of component 3. The ground-state analogue enzyme inhibitor purine riboside quenched emission associated with component 2 whereas the transition-state analogue inhibitor deoxycoformycin quenched emission from both components 2 and 3. The quenching due to inhibitor binding had no effect on the lifetimes or emission maxima of the decay-associated spectra. These observations can be explained by a simple model of four tryptophan environments. Quenching studies of the enzyme–inhibitor complexes indicate that adenosine deaminase undergoes different protein conformation changes upon binding of ground- and transition-state analogue inhibitors. The results are consistent with localized structural alterations in the enzyme.

Adenosine deaminase (EC 3.5.4.4), a purine salvage enzyme, catalyzes the conversion of adenosine and deoxyadenosine to inosine and deoxyinosine, respectively. Hereditary deficiency of adenosine deaminase is associated with a severe combined immunodeficiency (Giblett et al., 1972) which typically results in severe lymphopenia. The specific lympholytic effect of adenosine deaminase inhibitors has been exploited in the use of these compounds for chemotherapy, especially for certain leukemias that are associated with a marked increase in lymphocytes.

The structures of three adenosine deaminase inhibitors are shown in Figure 1. Ground-state or substrate analogue inhibitors, which include purine riboside, exhibit fast binding kinetics, resulting in instantaneous inhibition (Frieden et al., 1980). Transition-state analogue inhibitors, which resemble the proposed tetrahedral intermediate in the reaction catalyzed by adenosine deaminase, include 1,6-dihydro-6-(hydroxymethyl)purine riboside (DHMPR)[1] and the antibiotics coformycin and deoxycoformycin (Evans & Wolfenden, 1970; Agarwal et al., 1978). These inhibitors exhibit slow binding kinetics (Frieden et al., 1980). It is postulated that the slow binding kinetics are due to conformational changes in the protein, which result in formation of the transition-state complex. The rearrangements in the protein may occur in regions distant from the site. Alternatively, they may be confined to structural changes around the active site. Another potent inhibitor of adenosine deaminase, *erythro*-9-(hydroxy-3-nonyl)adenine (EHNA), which is classified as a competitive, ground-state analogue inhibitor, exhibits semislow binding kinetics (Frieden et al., 1980). Because EHNA is not deaminated by the enzyme, it has been proposed that EHNA binds at an auxiliary binding region near the active site (Woo

† This work was supported by Grants CA26391 and GM35009.
* Authors to whom correspondence should be addressed.

[1] Abbreviations: EHNA, *erythro*-9-(hydroxy-3-nonyl)adenine; DHMPR, 1,6-dihydro-6-(hydroxymethyl)purine riboside; NATA, *N*-acetyltryptophanamide; PBS, phosphate-buffered saline; TCE, trichloroethanol.

0006-2960/89/0428-2040$01.50/0

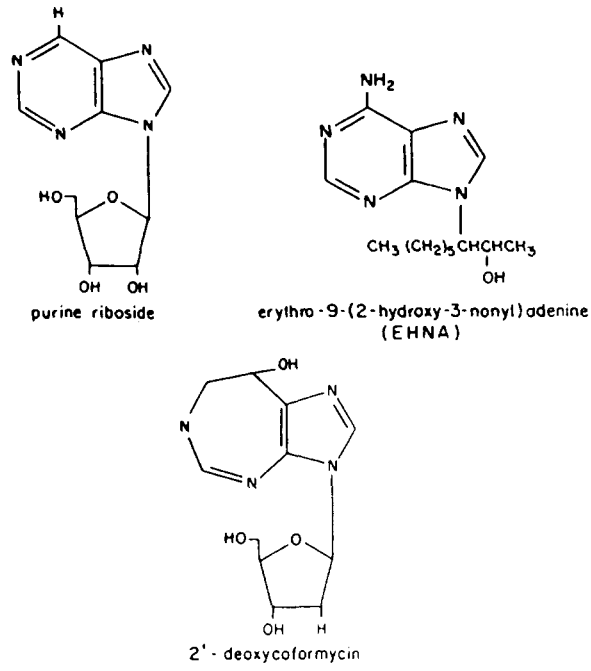

FIGURE 1: Structures of adenosine deaminase inhibitors.

& Baker, 1982). The distinction between ground- and transition-state analogue inhibitors has been blurred by a recent observation that C-6 of purine riboside is converted from sp^2 to sp^3 hybridization in the enzyme–inhibitor complex (Kurz & Frieden, 1987).

We have previously examined human adenosine deaminase by steady-state fluorescence spectroscopy (Philips et al., 1986). Human adenosine deaminase has four tryptophans (Wiginton et al., 1984; Dadonna et al., 1984). These studies showed that small solute quenchers shift the emission maximum of the intrinsic tryptophan fluorescence. The polar quenchers, iodide and acrylamide, cause a blue shift in the peak, whereas the nonpolar quencher trichloroethanol shifts the peak to the red. This indicates that the emission spectrum of adenosine deaminase is heterogeneous, involving contributions from tryptophan in at least two different environments. The Stern–Volmer constants from experiments with these quenchers reveal that the tryptophan environments in adenosine deaminase are relatively hydrophobic. Binding of the inhibitors purine riboside, deoxycoformycin, and DHMPR decreases the intrinsic fluorescence of adenosine deaminase, raising the possibility of tryptophan residue(s) near the active site. Corroborative evidence is provided by the fact that the fluorescence is not affected by binding of EHNA to the putative auxiliary site. Steady-state quenching experiments showed that the quenching parameters for the enzyme–inhibitor complexes differ from those for the uncomplexed enzyme. From these data it appears that the tryptophan environments are altered upon inhibitor binding, consistent with conformational changes in the protein upon binding both ground- and transition-state analogue inhibitors. However, for those inhibitors that decrease protein fluorescence, we cannot draw definite conclusions regarding protein structural changes.

Extension of the steady-state studies to time-resolved fluorescence experiments has the potential of yielding more detailed information about the tryptophan environments of adenosine deaminase. The emission spectrum of the enzyme may be resolved into component spectra corresponding to different tryptophan environments. In this paper, we describe the separation of the emission spectrum of adenosine deaminase into three lifetime components with at least two distinct emission maxima. The effects of solute quenchers and enzyme inhibitors on the decay-associated spectra were used to probe the quenching mechanisms as well as the number of distinguishable tryptophan environments. Finally, fluorescence quenching experiments were done on the enzyme–inhibitor complexes and were compared to those on the uncomplexed enzyme. Changes in the decay-associated spectra of components whose fluorescence was unaffected by inhibitor binding provided further evidence of protein conformational alterations.

Experimental Procedures

Materials

N-Acetyltryptophanamide (NATA) and purine riboside were purchased from Sigma Chemical Co. EHNA was purchased from Burroughs Wellcome Co. (Research Triangle Park, NC). Deoxycoformycin was a gift from the National Cancer Institute. DHMPR was kindly provided by Dr. R. Wolfenden and was stored under nitrogen. A fluorescent impurity that forms in the DHMPR preparation upon exposure to air was removed by chromatography on a SiO_2 column under nitrogen using 30% (v/v) methanol in chloroform. Acrylamide purchased from Bio-Rad Laboratories was recrystallized from ethyl acetate, and stock solutions of 8 M acrylamide were made. Ethylene glycol (99+%) and trichloroethanol were from Aldrich Chemical Co. Stock solutions of 1 M trichloroethanol in ethylene glycol were made. All other chemicals were reagent grade or higher. Phosphate-buffered saline (PBS) was 0.85 mM Na_2HPO_4, 0.18 mM NaH_2PO_4, and 0.14 M NaCl (pH 7.4). Stock solutions of 1 M KI in PBS contained a trace of thiosulphate to retard I_3^- formation.

Adenosine deaminase was purified from human thymus on an immunoaffinity column constructed from a monoclonal antibody to human adenosine deaminase (Philips et al., 1986). Protein concentration was determined by the method of Lowry et al. (1951), and a molecular weight of 41 000 was assumed. The purified enzyme was diluted to a concentration of 7–10 μM in PBS and was clarified by centrifugation prior to use. For the iodide quenching experiments, the enzyme was dialyzed into PBS containing 1 M KCl to maintain constant ionic strength. No changes in adenosine deaminase activity were observed in the presence of 1 M acrylamide, 1 M KI, 1 M KCl, or 300 mM trichloroethanol when assayed at saturating concentrations of substrate. Calf intestinal adenosine deaminase was purchased from Sigma Chemical Co. and was diluted to 7–10 μM in PBS.

Methods

Spectral Measurements. All steady-state fluorescence measurements were made on an SLM-8000 photon-counting spectrofluorometer interfaced to an Apple II+ microcomputer. Excitation was selected by a single monochromator at 296 nm (4-nm band-pass), and emission was scanned from 300 to 400 nm (16-nm band-pass). The excitation and emission polarizers were oriented at 55° and 0°, respectively. Steady-state fluorescence data were collected as a ratio of emission to lamp reference and were corrected for wavelength-dependent instrument response. All experiments were performed at 10 °C to prevent denaturation of the enzyme during acquisition of lifetime data. Absorbance was measured on a Cary 219 spectrophotometer.

Time-Resolved Fluorescence Measurements. Fluorescence lifetimes were measured in a Photochemical Research Associates nanosecond fluorometer with a T optical design. Since the counting rate in time-correlated single photon counting is low (about 2% of the lamp repetition rate), the two detectors

share the time-to-amplitude converter. A decision/coincidence circuit determines which detector received the signal and routes it to the appropriate decay curve in a Tracor Northern TN-1750 multichannel analyzer with 2K memory. The flash lamp was filled with 1.5 atm of nitrogen and operated at 20–25 kHz with 5 kV applied across a 1.5-mm electrode gap. Under these conditions the pulse width was about 1.7 ns fwhm. Excitation at 296 nm was selected by a microCoatings (Westford, MA) interference filter (10-nm band-pass). Since the incident light was unpolarized, a single polarizer oriented at 35° was used on the emission side. Emission wavelengths were selected by Instruments SA H-10 monochromators (16-nm band-pass). Fluorescence decays were acquired in T-format by alternating between a fluorescent sample and a reference fluorophore for the instrument response. Sample and reference decay curves were collected simultaneously at two emission wavelengths and were stored in 512 channels of 0.108 ns/channel. Data acquisition was controlled by a Digital Equipment Corp. MINC-11 computer. A solution of terphenyl in 80% ethanol and 0.8 M KI (containing a trace of thiosulfate to retard I_3^- formation) was used as the reference fluorophore. A lifetime of 0.25 ± 0.01 ns for the quenched terphenyl was determined in separate experiments using NATA in PBS as the monoexponential standard.

Time-Resolved Emission Spectroscopy. Fluorescence decay measurements were made at six different emission wavelengths: 320–370 nm in 10-nm intervals. The sample dwell time was 100 s/cycle, and the experiment was continued until the sample decay curve contained approximately 10000 counts in the peak. For each measurement, the absorbance of both the enzyme and reference fluorophore was less than 0.1 at 296 nm with 4-mm path length. Time-resolved fluorescence measurements were made on adenosine deaminase in the absence and presence of quenchers: 25, 50, 100, and 200 mM acrylamide or iodide; 25 mM trichloroethanol. Quenching experiments were also performed on adenosine deaminase in the presence of saturating concentrations of three inhibitors: purine riboside (1 mM), EHNA (20 μM), and deoxycoformycin (20 μM). The steady-state emission spectrum of the sample was taken before and after each addition, and a new set of decay measurements was made. Blanks containing buffer and quencher were acquired for the same length of time as the enzyme sample. The acquisition of time-resolved emission spectral data at six wavelengths took over 6 h for enzyme alone, and considerably longer in the presence of quenchers and inhibitors. Fluorescence decay measurements were made on a monoexponential fluorescent compound (NATA in PBS) before each set of experiments to check instrumental performance. Data acquisition for the standard was continued until about 15000 counts were in the peak. The fluorescence lifetime of NATA at 10 °C was 3.40 ± 0.05 with χ_r^2 values of about 1.0–1.2.

The fluorescence decay curves were deconvolved by using the reference decay instead of a lamp profile in a modified least-squares analysis (Kolber & Barkley, 1986) based on the Marquardt algorithm (Bevington, 1969). Each sample decay curve was deconvolved by using the reference decay acquired at the same detector. Goodness of fit was evaluated from the value of reduced χ_r^2 and the shape of the autocorrelation function of the weighted residuals (Grinvald & Steinberg, 1974). The data were fitted to a sum of exponentials plus a term for scattered light:

$$I(\lambda,t) = \sum_i \alpha_i(\lambda) \exp(-t/\tau_i) + a(\lambda)\,\delta(t) \qquad (1)$$

where $\alpha_i(\lambda)$ is the preexponential weighting factor at wavelength λ and τ_i is the fluorescence lifetime for component i; $a(\lambda)$ is the amount of light scattered at wavelength λ. The reference lifetime was treated as an adjustable parameter in analyses of the monoexponential standard. However, its value was fixed at 0.25 ns in analyses of adenosine deaminase decays. The fluorescence decays acquired at different emission wavelengths were deconvolved by single-curve analysis and by multiple-curve analysis in a global program (Knutson et al., 1983). The global analysis assumes that the lifetimes but not the preexponential factors and scattered light is independent of wavelength.

The decay-associated spectra, which are the fluorescence spectra that each lifetime component would have in the absence of the others, were derived by combining time-resolved and steady-state data:

$$I_i(\lambda) = I(\lambda)[\alpha_i(\lambda)\tau_i/\sum_i \alpha_i(\lambda)\tau_i] \qquad (2)$$

where $I_i(\lambda)$ is the intensity due to component i and $I(\lambda)$ is the corrected steady-state intensity at wavelength λ. The steady-state and time-resolved measurements were made in different instruments at the same emission band-pass. However, the excitation trains as well as the stray light rejection characteristics of the emission monochromators differ in the two instruments. The amount of scattered light in the steady-state intensity measurements was probably much less than the value of $a(\lambda)$ estimated from time-resolved data. The $a(\lambda)$ values were typically 3–6% of the total intensity and thus had only minor effects on the decay-associated spectra. The integrated intensities I_i of the decay-associated spectra from 320 to 370 nm were calculated by the trapezoidal rule. The centers of gravity $\nu_{cg,i}$ (in nm^{-1}) of the decay-associated spectra were calculated from (Lakowicz & Hogen, 1981)

$$\nu_{cg,i} = \sum_j I_i(\lambda_j)\lambda_j^{-3}/\sum_j I_i(\lambda_j)\lambda_j^{-2} \qquad (3)$$

where the wavelength λ_j goes from 320 to 370 nm in 10-nm intervals.

The apparent Stern–Volmer constant K_{svi}(app) of component i was calculated from the intensity quenching of the decay-associated spectrum:

$$I_{0i}/I_i = 1 + K_{svi}(\text{app})[Q] \qquad (4)$$

where I_{0i} and I_i are the integrated intensities in the absence and presence of low concentrations of quencher Q. Here K_{svi}(app) includes contributions from dynamic K_{svi} and static V_i quenching constants (Lakowicz, 1983):

$$K_{svi}(\text{app}) = K_{svi} + V_i \qquad (5)$$

The Stern–Volmer constant K_{svi} for dynamic quenching was calculated from

$$\tau_{0i}/\tau_i = 1 + K_{svi}[Q] \qquad (6)$$

where τ_{0i} and τ_i are the lifetimes in the absence and presence of quencher. The values of K_{svi}(app) and K_{svi} were estimated from eq 4 and 6 by linear regression of the data for four quencher concentrations.

Results

Time-Resolved Emission Spectroscopy of Adenosine Deaminase. Time-resolved spectral data were acquired at six emission wavelengths between 320 and 370 nm (10-nm intervals). The decay curves were deconvolved by single-curve analysis of the data at each wavelength and global analysis of data for six emission wavelengths. The fluorescence decay data were fitted to two- and three-exponential functions with and without the correction for scattered light (Kolber & Barkley, 1986). In all cases the χ_r^2 values were lower for three-exponential than for two-exponential fits. Moreover, the partial χ_r^2 values for individual decay curves in a global

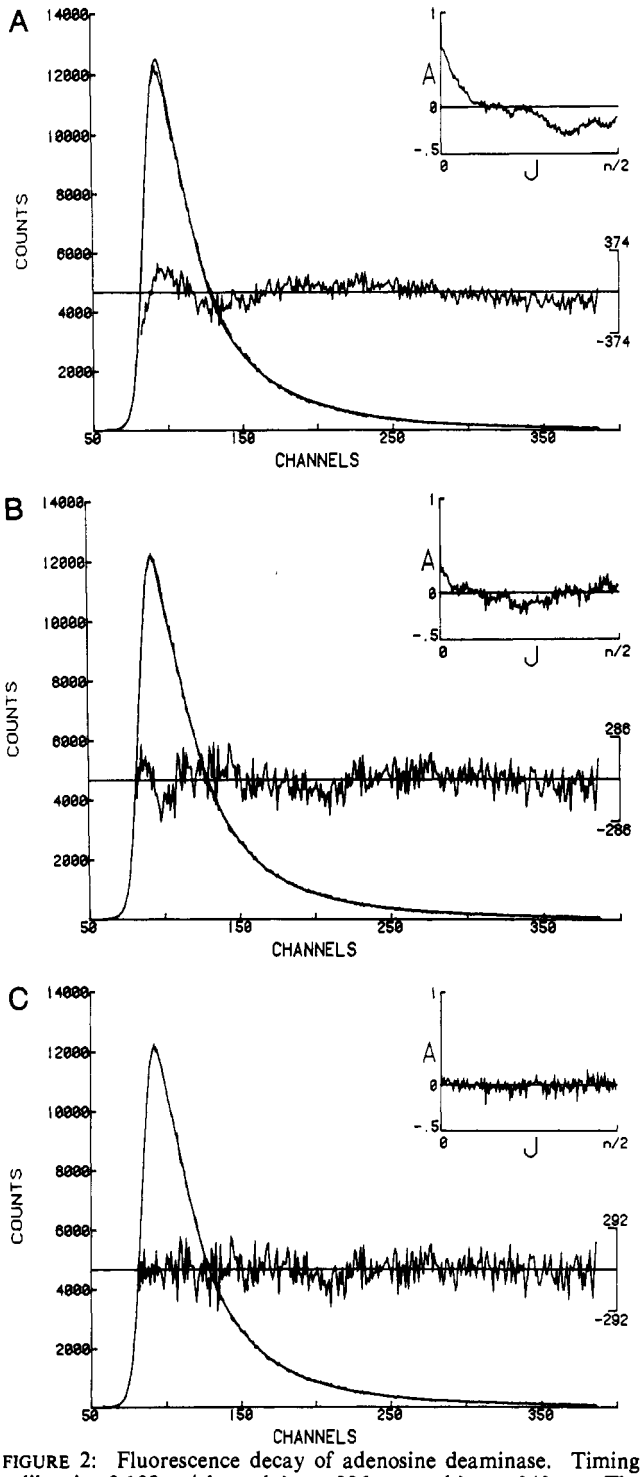

FIGURE 2: Fluorescence decay of adenosine deaminase. Timing calibration 0.108 ns/channel, λ_{ex} = 296 nm, and λ_{em} = 340 nm. The data were fit by global analysis of decay curves at six emission wavelengths (320–370 nm at 10-nm intervals) to the following: (A) Two exponentials; $\alpha_1 = 0.321$, $\tau_1 = 1.41$ ns, $\alpha_2 = 0.094$, $\tau_2 = 5.30$ ns; partial $\chi_r^2 = 2.79$. (B) Three exponentials; $\alpha_1 = 0.247$, $\tau_1 = 0.37$ ns, $\alpha_2 = 0.235$, $\tau_2 = 2.31$, $\alpha_3 = 0.049$, $\tau_3 = 6.45$ ns; partial $\chi_r^2 = 1.37$. (C) Three exponentials plus term for scattered light: $\alpha_1 = 0.209$, $\tau_1 = 1.16$ ns, $\alpha_2 = 0.150$, $\tau_2 = 3.24$ ns, $\alpha_3 = 0.026$, $\tau_3 = 7.59$, $a = 0.023$; partial $\chi_r^2 = 0.91$. Values of preexponential factors normalized to steady-state intensity at 340 nm. The percent residuals and autocorrelation function (insert) are also shown.

analysis were about the same as the χ_r^2 values obtained from single-curve analyses. This implies that the lifetimes of adenosine deaminase are independent of wavelength, as assumed in the global program. Figure 2 compares the theoretical fits from global analyses assuming two- and three-exponential decays for adenosine deaminase in PBS. The two-

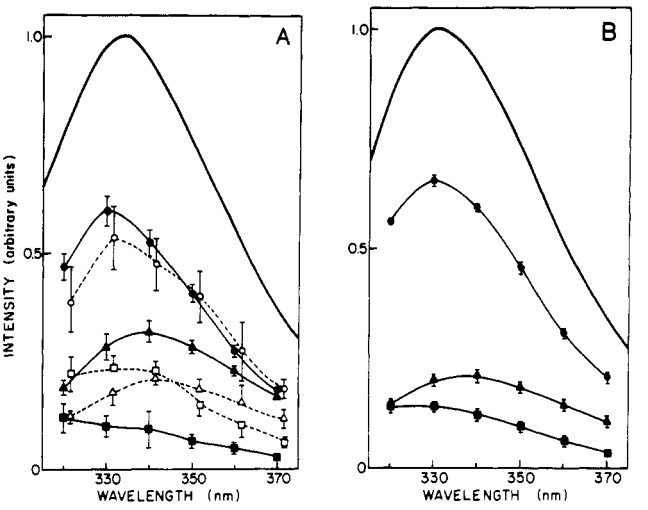

FIGURE 3: Decay-associated emission spectra of adenosine deaminase. (A) Heavy solid line: steady-state spectrum of adenosine deaminase in PBS. Steady-state contributions from (■, □) component 1, (●, ○) component 2, and (▲, △) component 3 constructed from decay parameters in Table I. Filled symbols, solid lines: decay parameters uncorrected for scattered light. Open symbols, dashed lines: decay parameters corrected for scattered light displaced 3 nm to the right to avoid overlap of error bars. Error bars are propagated errors from Table I. (B) Heavy solid line: steady-state spectrum of adenosine deaminase in PBS containing 1 M KCl. Steady-state contributions from (■) component 1, (●) component 2, and (▲) component 3 constructed from decay parameters in Table II. Error bars are propagated errors from Table II.

exponential fit gives lifetimes of 1.4 and 5.3 ns, but the global $\chi_r^2 = 3.3$ and the poor shape of the autocorrelation function are clearly unacceptable (Figure 2A). For the three-exponential fit, the lifetimes were 0.4, 2.3, and 6.5 ns; the global $\chi_r^2 = 1.45$ and the autocorrelation function were improved (Figure 2B). The existence of a short fluorescence lifetime was established by ruling out instrumental artifacts and by adding a term for scattered light in the data analysis. The χ_r^2 values dropped to <1.5 in both single- and multiple-curve analyses assuming a two-exponential function with scattered light. For the data in Figure 2, the global $\chi_r^2 = 1.49$ was about the same as the value for the three-exponential fit without scatter correction, but the autocorrelation function was slightly worse (not shown). Inclusion of the scattered light term in the analysis for three exponentials gave lifetimes of 1.2, 3.2, and 7.6 ns; the global $\chi_r^2 = 1.03$ and the autocorrelation function fluctuated randomly around zero (Figure 2C). The stray light contamination varied with emission wavelength from 7% of the intensity at 320 nm to 1.5% at 370 nm. Attempts to eliminate the stray light contribution from the data by subtracting blanks without protein were ineffective. The 1-ns lifetime of the short-lived fluorescence decay was supported by experiments on adenosine deaminase in PBS containing 1 M KCl. These data gave excellent fits to three- but not two-exponential functions with χ_r^2 values of about 1.1 and lifetimes of 1.0, 2.4, and 6.3 ns. Inclusion of the scattered light term in the analysis had little effect on χ_r^2 and on the $\alpha_i(\lambda)$ and τ_i values; it frequently gave unphysical negative values for the amount of scattered light. Thus, we conclude that the adenosine deaminase fluorescence decay is described by at least three exponential functions.

Tables I and II summarize the time-resolved data for the various emission wavelengths. The preexponential weighting factors $\alpha_i(\lambda)$ represent the emission spectra of the individual components. Figure 3A presents the steady-state spectrum of adenosine deaminase in PBS and the decay-associated spectra of the three components constructed according to eq

Table I: Fluorescence Decay Parameters of Adenosine Deaminase in PBS[a]

λ_{em} (nm)	$\alpha_1(\lambda)$	$\alpha_2(\lambda)$	$\alpha_3(\lambda)$	a
320	0.44 ± 0.09	0.208 ± 0.009	0.030 ± 0.002	
	(0.20 ± 0.01)	(0.13 ± 0.02)	(0.02 ± 0.02)	0.05 ± 0.01
330	0.37 ± 0.05	0.264 ± 0.005	0.044 ± 0.006	
	(0.22 ± 0.01)	(0.18 ± 0.02)	(0.025 ± 0.004)	0.04 ± 0.01
340	0.4 ± 0.1	0.237 ± 0.007	0.051 ± 0.003	
	(0.195 ± 0.009)	(0.16 ± 0.01)	(0.029 ± 0.004)	0.03 ± 0.01
350	0.24 ± 0.03	0.183 ± 0.003	0.045 ± 0.002	
	(0.14 ± 0.01)	(0.13 ± 0.01)	(0.026 ± 0.004)	0.029 ± 0.009
360	0.18 ± 0.04	0.123 ± 0.002	0.036 ± 0.001	
	(0.10 ± 0.02)	(0.10 ± 0.02)	(0.023 ± 0.005)	0.019 ± 0.004
370	0.08 ± 0.01	0.082 ± 0.001	0.027 ± 0.001	
	(0.057 ± 0.003)	(0.061 ± 0.003)	(0.016 ± 0.002)	0.007 ± 0.003
τ_i (ns)	0.27 ± 0.05	2.23 ± 0.05	6.3 ± 0.1	
	(1.1 ± 0.1)	(3.1 ± 0.2)	(7.3 ± 0.3)	

[a] Data from 10 experiments. The $\alpha_i(\lambda)$ and $a(\lambda)$ values are scaled to the steady-state intensity $I(\lambda)$. Values enclosed in parentheses are corrected for scattered light.

Table II: Fluorescence Decay Parameters of Adenosine Deaminase in PBS Containing 1 M KCl[a]

λ_{em} (nm)	$\alpha_1(\lambda)$	$\alpha_2(\lambda)$	$\alpha_3(\lambda)$
320	0.14 ± 0.01	0.24 ± 0.01	0.023 ± 0.001
330	0.142 ± 0.007	0.279 ± 0.006	0.032 ± 0.001
340	0.12 ± 0.01	0.25 ± 0.01	0.034 ± 0.001
350	0.094 ± 0.007	0.193 ± 0.006	0.030 ± 0.001
360	0.062 ± 0.006	0.131 ± 0.006	0.023 ± 0.001
370	0.034 ± 0.003	0.087 ± 0.003	0.016 ± 0.001
τ_i (ns)	1.01	2.36	6.3

[a] Global analysis of data from four experiments. The $\alpha_i(\lambda)$ values are scaled to the steady-state intensity $I(\lambda)$.

2 from the decay parameters in Table I. The light solid curves are the decay-associated spectra computed from the $\alpha_i(\lambda)$ and τ_i values uncorrected for scattered light. Component 2 with lifetime τ_2 = 2.2 ns has an emission maximum at about 330 nm and contributes about 55% of the intensity. Component 3 with lifetime τ_3 = 6.3 ns has a peak at about 340 nm and contributes about 35% of the intensity. The short-lifetime component 1 amounts to only 10% of the intensity. The dashed curves represent the decay-associated spectra computed from the decay parameters corrected for scattered light. For components 2 and 3, the shapes of the decay-associated spectra are not affected by the presence of scattered light. However, component 1 begins to resemble an emission spectrum with a maximum around 330 nm after removal of the scattered light. The fractional intensity of component 2 remains about the same, but the relative contributions of components 1 and 3 change. Moreover, the uncertainties in the values of the decay parameters for components 2 and 3 but not component 1 are greater for analyses with the scattered light correction (Table I). The advantages of overdetermination accrued by global analysis may be somewhat compromised by the addition of another adjustable parameter. For our experimental conditions, better resolution of a four-component decay (three exponentials plus scatter) probably requires a larger data set. Since only component 1 is significantly distorted by the stray light, we have more confidence in the $\alpha_i(\lambda)$ and τ_i values for components 2 and 3 obtained without the scattered light term in the analysis. In subsequent discussions, we will emphasize the results for components 2 and 3 which are not corrected for scattered light and the results for component 1 which are corrected for scattered light. Except for component 1, the qualitative trends and conclusions are not influenced by the light scattering of the protein sample.

Figure 3B shows the results for adenosine deaminase in PBS containing 1 M KCl. The fluorescence lifetimes in the presence of 1 M KCl (Table II) are essentially identical with the corrected value of τ_1 and the uncorrected values of τ_2 and τ_3 in PBS (Table I). The lower values of $\alpha_1(\lambda)$ are due to the absence of scattered light. The steady-state emission maximum (heavy solid curve) has shifted to 330 from 335 nm with no change in the maxima of the decay-associated spectra: components 1 and 2 have peaks at about 330 nm, and component 3 has a peak at about 340 nm. However, the fractional intensities of components 2 and 3 are somewhat different: component 2 contributes about 65% but component 3 contributes only about 25% in high salt. It appears that some of the intensity from component 3 has transferred to component 2. This would account for the blue shift in the steady-state spectrum.

Effects of Quenchers on Decay-Associated Spectra of Adenosine Deaminase. Low concentrations of solute quenchers of different polarity were used to probe the tryptophan environments of adenosine deaminase. Acrylamide is a polar, neutral quencher that quenches solvent-accessible residues efficiently (Eftink & Ghiron, 1981). Iodide is an ionic quencher that quenches mainly surface residues in a polar environment (Lakowicz, 1983), while trichloroethanol is a nonpolar quencher that senses hydrophobic environments and causes exaggerated quenching (Eftink et al., 1977). These compounds appear to quench indole fluorescence with an efficiency near unity, as defined by the ratio of the apparent quenching rate constant to the diffusion-limited rate constant calculated from the time-independent portion of the von Somoluchowski equation (Eftink & Ghiron, 1981). Time-resolved data were acquired at six emission wavelengths for adenosine deaminase in the absence and presence of various concentrations of quencher. For each quencher concentration, $\alpha_i(\lambda)$ and τ_i values were determined by global analysis and a set of decay-associated spectra were constructed. In all cases three exponential components were required to fit the data. Attempts to resolve a fourth exponential component were unsuccessful.

Figure 4 summarizes the acrylamide and iodide quenching studies of adenosine deaminase. The three lifetime components were accessible to both of the quenchers. The upper histogram shows the centers of gravity of the three decay-associated spectra at four concentrations of quencher. The emission spectrum of component 3 shifted progressively to the blue with increasing acrylamide concentration. This indicates that component 3 comprises at least two tryptophan environments: the red-shifted emission is more accessible to acrylamide than the blue-shifted emission. The middle histogram displays the intensity decreases of the decay-associated spectra. Component 1 is slightly more sensitive to acrylamide than components 2

Table III: Effects of Enzyme Inhibitors on Decay-Associated Emission of Adenosine Deaminase[a]

inhibitor	I_1[b]	I_2[c]	I_3[c]
none	1.0	1.0	1.0
EHNA	0.97	0.97	0.97
PR	0.99	0.81	0.94
dCF	0.98	0.57	0.68

[a] Relative integrated fluorescence intensities. [b] Spectrum of component 1 was constructed from decay parameters corrected for scattered light. [c] Spectra of components 2 and 3 were constructed from decay parameters uncorrected for scattered light.

and 3. The apparent Stern–Volmer constants for acrylamide quenching are about 9 M^{-1} for component 1 and 7–8 M^{-1} for components 2 and 3. Since the intensities of components 1 and 2 did not increase, the observed quenching does not appear to involve substantial transfer of emission from a longer to a shorter lifetime component. As seen in the lower histogram, acrylamide also caused decreases in the three fluorescence lifetimes. The Stern–Volmer constants calculated from the lifetime drops, about 4 M^{-1} for component 1 and about 2 M^{-1} for components 2 and 3, are lower than the values calculated from the intensity drops. Thus, there appears to be some static quenching by acrylamide. The iodide quenching data paralleled the acrylamide results, but the extent of quenching was somewhat less for components 2 and 3.

Adenosine deaminase fluorescence was extensively quenched by 25 mM trichloroethanol: components 1 and 2 about 30% and component 3 about 40% (not shown). The center of gravity of the decay-associated spectrum of component 3 stayed at 342 nm, indicating that trichloroethanol does not quench the red-shifted emission. Addition of 25 mM trichloroethanol had no effect on the lifetimes of adenosine deaminase within experimental error. Previous steady-state results show that adenosine deaminase fluorescence is much more sensitive to quenching by trichloroethanol than acrylamide or iodide (Philips et al., 1986). The Stern–Volmer plot for trichloroethanol quenching of the enzyme alone exhibits strong upward curvature, the hallmark of static quenching. However, even in the presence of 300 mM trichloroethanol with only 6% of the steady-state intensity remaining, the red-shifted emission persists as evident from the maximum at 342 nm. The high degree of static quenching at a low concentration of trichloroethanol confirms the hydrophobic nature of some of the tryptophan environments in adenosine deaminase.

Effect of Inhibitors on Decay-Associated Spectra of Adenosine Deaminase. The binding of enzyme inhibitors also quenches adenosine deaminase fluorescence (Philips et al., 1986). Purine riboside, deoxycoformycin, and DHMPR quench the emission to different extents, whereas EHNA has

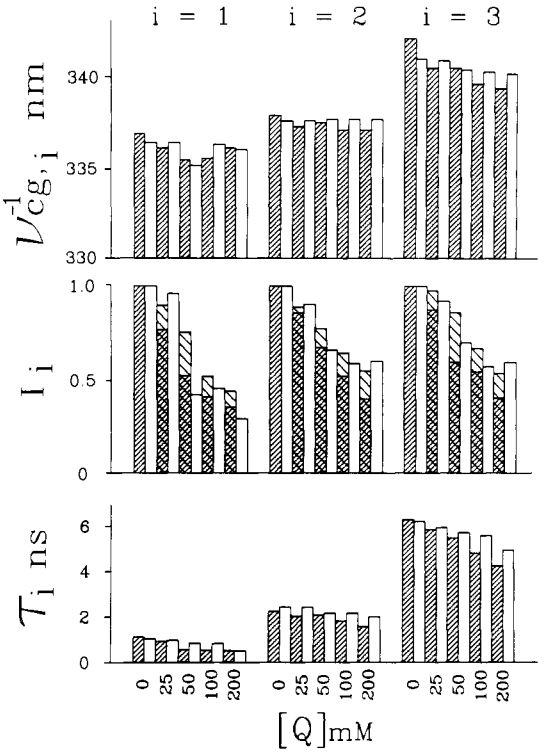

FIGURE 4: Effects of acrylamide and KI on decay-associated emission of adenosine deaminase and adenosine–EHNA complex. Quenching of adenosine deaminase by (right-slanted hatched bars) acrylamide or (□) KI. Quenching of adenosine deaminase–EHNA complex with acrylamide (left-slanted hatched bars). Upper histogram: centers of gravity of the decay-associated spectra. Middle histogram: relative integrated fluorescence intensities of the decay-associated spectra. Lower histogram: fluorescence lifetimes. For acrylamide, spectrum of component 1 was constructed from decay parameters corrected for scattered light; spectra of components 2 and 3 were constructed from decay parameters uncorrected for scattered light.

no apparent effect (0–2%). We therefore looked at the effects of inhibitor binding on the decay-associated spectra. For each enzyme–inhibitor complex a new set of decay-associated spectra were constructed and compared to those of the enzyme alone. Table III shows the intensities of the decay-associated spectra for EHNA, purine riboside, and deoxycoformycin complexes relative to the enzyme alone. Component 1 was unaffected by inhibitor binding. Component 2 was quenched about 20% by purine riboside and about 40% by deoxycoformycin, but was not quenched by EHNA. Component 3 was quenched about 30% by deoxycoformycin with no shift in the center of gravity of the decay-associated spectrum, suggesting that the red-shifted environment is not quenched by the inhibitor. Table IV gives the preexponential factors at 330 nm and the lifetimes for the enzyme–inhibitor complexes. The

Table IV: Effect of Inhibitors on Fluorescence Decay Parameters of Adenosine Deaminase[a]

inhibitor	α_1(330 nm)	τ_1 (ns)	α_2(330 nm)	τ_2 (ns)	α_3(330 nm)	τ_3 (ns)	a(330 nm)
human							
none[b]	0.37 ± 0.05	0.27 ± 0.05	0.264 ± 0.005	2.23 ± 0.05	0.044 ± 0.006	6.3 ± 0.1	
	(0.22 ± 0.01)	(1.1 ± 0.1)	(0.18 ± 0.02)	(3.1 ± 0.2)	(0.025 ± 0.004)	(7.3 ± 0.3)	0.04 ± 0.01
EHNA[c]	0.35 ± 0.04	0.33 ± 0.04	0.252 ± 0.007	2.29 ± 0.05	0.041 ± 0.002	6.5 ± 0.1	
	(0.223 ± 0.001)	(0.99 ± 0.05)	(0.177 ± 0.009)	(2.97 ± 0.09)	(0.026 ± 0.001)	(7.27 ± 0.16)	0.040 ± 0.002
purine riboside[c]	0.30 ± 0.03	0.37 ± 0.08	0.22 ± 0.01	2.2 ± 0.2	0.039 ± 0.006	6.4 ± 0.4	
	(0.22 ± 0.02)	(1.0 ± 0.2)	(0.14 ± 0.02)	(3.1 ± 0.4)	(0.022 ± 0.008)	(7.3 ± 0.8)	0.032 ± 0.002
deoxycoformycin[c]	0.384 ± 0.006	0.36 ± 0.02	0.15 ± 0.01	2.11 ± 0.08	0.030 ± 0.003	6.1 ± 0.2	
	(0.27 ± 0.02)	(0.88 ± 0.08)	(0.091 ± 0.006)	(3.4 ± 0.2)	(0.009 ± 0.001)	(8.0 ± 0.2)	0.033 ± 0.008
calf							
none	0.21	1.1	0.20	2.67	0.033	6.6	
deoxycoformycin	0.24	0.98	0.09	2.82	0.017	6.4	

[a] The α_i and a values are scaled to the steady-state intensity at 330 nm. Values enclosed in parentheses are corrected for scattered light. [b] Data from Table I. [c] Average of data from two experiments.

Table V: Qualitative Effects of Inhibitors and Solute Quenchers on Adenosine Deaminase Fluorescence

lifetime component	inhibitor[a]	quencher	
		acrylamide	KI
1	none	+++	+++
2	PR (+) dCF (+++)	++	+
3A	dCF (++)	none[c]	none[c]
3B	none[b]	++	+

[a] Purine ribosine (PR); deoxycoformycin (dCF). [b] Decay-associated spectrum not shifted. [c] Decay-associated spectrum blue shifted.

decay parameters were not affected by EHNA, and the lifetimes were not changed by purine riboside and deoxycoformycin. The decreases in the values of α_2 and α_3 account for the intensity drops upon binding of purine riboside and deoxycoformycin. Kurz et al. (1985) postulated that the fluorescence quenching of calf intestinal adenosine deaminase caused by deoxycoformycin is due to energy transfer. Our observation that the lifetimes did not decrease and that the preexponential factors of the shorter lifetime components did not increase appears to rule out energy transfer in the case of the human enzyme. We also made a few time-resolved spectral measurements on calf adenosine deaminase (Table IV). In the presence of deoxycoformycin the lifetimes of the calf enzyme were also unchanged and the α_2 and α_3 values were decreased. These results suggest that binding of deoxycoformycin decreases protein fluorescence by static quenching rather than by energy transfer in both calf and human adenosine deaminases. We were unable to make accurate fluorescence decay measurements on the enzyme–DHMPR complex, because of a minor fluorescent impurity persisting in the DHMPR preparation.

The qualitative effects of inhibitors and solute quenchers on the time-resolved emission spectroscopy of adenosine deaminase provide additional information about the tryptophan environments in the protein. A proposed model for the tryptophan environments is summarized in Table V. The inhibitor binding experiments distinguish three tryptophan environments: component 1, which is not quenched by inhibitors; component 2, which is quenched by both purine riboside and deoxycoformycin; and component 3, which is only quenched significantly by deoxycoformycin. The acrylamide quenching experiments reveal that component 3 can be split into two distinct spectral environments: component 3A is less sensitive to acrylamide than component 3B. Component 3B appears to be the most polar environment with a red-shifted emission spectrum. The changes in adenosine deaminase fluorescence upon binding of the ground- and transition-state analogue inhibitors are different. Although both purine riboside and deoxycoformycin quench emission from component 2, deoxycoformycin has a much larger effect. Since both inhibitors bind at the enzyme active site, this tryptophan environment may be near the active site. The fact that EHNA has no effect on component 2 supports the proposal of Woo and Baker (1982) that EHNA does not bind directly at the active site but at an auxiliary "EHNA-binding" region. The quenching of component 2 by purine riboside and deoxycoformycin may also be due to long-range protein conformation changes.

Effects of Quenchers on Decay-Associated Spectra of Enzyme–Inhibitor Complexes. So far, we have obtained evidence supporting four tryptophan environments in adenosine deaminase, two of which are affected by inhibitor binding. Steady-state fluorescence quenching studies showed that the quenching parameters for enzyme–inhibitor complexes differed from those for the enzyme alone (Kurz et al., 1985; Philips et al., 1986). However, interpretation of the differences in terms of protein structural changes is ambiguous for those inhibitors that quench the protein fluorescence. The time-resolved fluorescence quenching studies of the enzyme–inhibitor complexes provide more definitive information.

Since EHNA has no appreciable effect on the protein fluorescence, the emission from different tryptophan environments is presumably the same in the complexed and uncomplexed enzyme. In this case changes in accessibility to external quenchers can be examined for each lifetime component. The fluorescence intensities of the decay-associated spectra of the enzyme–EHNA complex quenched by acrylamide are shown in Figure 4. EHNA binding decreases the acrylamide quenching of all three components somewhat. The apparent Stern–Volmer constants drop 20–30% to about 7 M^{-1} for component 1 and about 5 M^{-1} for components 2 and 3. The centers of gravity of the decay-associated spectra of components 1 and 2 do not change, but the center of gravity of component 3 shifts slightly to the blue with increasing quencher concentration (not shown), indicating that the polar environment 3B is still accessible to acrylamide in the enzyme–EHNA complex. On the other hand, dynamic quenching of the three components appears to be about the same in the presence and absence of EHNA (K_{sv1} = 4 M^{-1}, K_{sv2} and K_{sv3} = 2 M^{-1}; not shown). Therefore, the decreased accessibility of the enzyme–EHNA complex appears to be due to a reduction in the extent of static quenching by acrylamide. This implies small conformation changes in the protein which affect the local environment of tryptophan residues. Binding of EHNA protected component 1 from iodide quenching: K_{sv1} dropped from about 4 M^{-1} to <1 M^{-1} in the presence of EHNA but had no effect on the quenching of components 2 and 3 (not shown). Trichloroethanol (25 mM) also quenched all three components in the enzyme–EHNA complex (not shown): component 1 somewhat more (40%) and components 2 and 3 slightly less (25% and 35%) than in the enzyme alone.

Interpretation of quenching data for the other enzyme–inhibitor complexes is hampered by the fact that inhibitor binding decreases the protein fluorescence: about 10% for purine riboside and 30% for deoxycoformycin. Quenching studies on these complexes probe the remaining emission. For those lifetime components unaffected by inhibitor, changes in quenching compared to the enzyme alone correspond to differences in susceptibility to quencher. As we showed in the preceding section, component 1 is not quenched by any of the inhibitors and component 3 is only quenched significantly by deoxycoformycin. Thus, the quenching patterns of component 1 may distinguish protein conformation changes caused by the three inhibitors. Likewise, component 3 will reveal differences between the two types of ground-state analogue inhibitors: EHNA and purine riboside.

Figure 5 shows the centers of gravity and fluorescence intensities of the decay-associated spectrum for component 1 of the enzyme–inhibitor complexes in the presence of various concentrations of acrylamide. Quenching of component 1 in the complexes is different from the enzyme alone. The enzyme–purine riboside complex is much more susceptible to acrylamide concentrations below 200 mM [K_{sv1}(app) = 40 M^{-1}] than either the EHNA [K_{sv1}(app) = 7 M^{-1}] or deoxycoformycin [K_{sv1}(app) <1 M^{-1}] complexes. Quenching of the purine riboside complex causes a slight blue shift in the center of gravity of component 1. However, at 200 mM acrylamide the intensity increases and the center of gravity jumps from 334 to 340 nm. Such an intensity increase coupled with a spectral shift may reflect transfer of some emission from

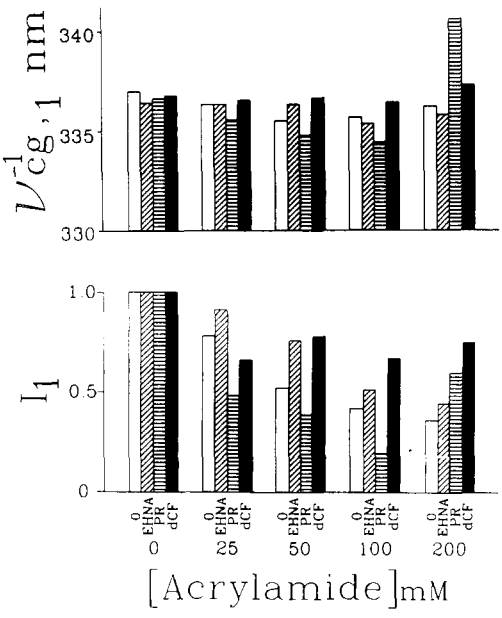

FIGURE 5: Acrylamide quenching of component 1 in adenosine deaminase–inhibitor complexes. Quenching in the (□) absence and presence of (slanted hatched bars) EHNA, (horizontal hatched bars) purine riboside (PR), and (■) deoxycoformycin (dCF). Upper histogram: centers of gravity of decay-associated spectra. Lower histogram: relative integrated fluorescence intensities of decay-associated spectra. Spectra were constructed from decay parameters corrected for scattered light. Data for adenosine deaminase alone from Figure 4.

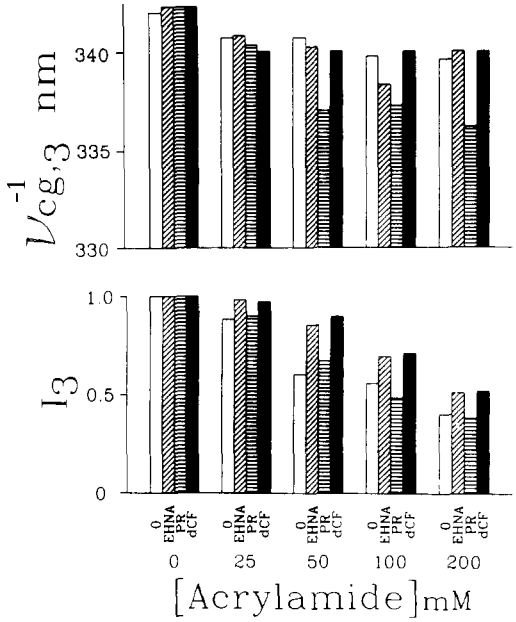

FIGURE 6: Acrylamide quenching of component 3 in adenosine deaminase–inhibitor complexes. Quenching in the (□) absence and presence of (slanted hatched bars) EHNA, (horizontal hatched bars) purine riboside (PR), and (■) deoxycoformycin (dCF). Upper histogram: centers of gravity of decay-associated spectra. Lower histogram: relative integrated fluorescence intensities of decay-associated spectra. Data for adenosine deaminase alone from Figure 4.

component 3 to component 1 due to dynamic quenching of the 6.3-ns lifetime down to about 1 ns. This is supported by a large blue shift in the center of gravity of component 3 in the purine–riboside complex (see Figure 6). The dynamic quenching by acrylamide (not shown) is also greater for the enzyme–purine riboside complex (K_{sv1} = 14 M^{-1}) than for enzyme alone (K_{sv1} = 4 M^{-1}). Since purine riboside binding alters both static and dynamic quenching, the protein conformation change probably encompasses the local tryptophan environment as well as larger distances affecting quencher penetration. The enzyme–deoxycoformycin complex is more susceptible to iodide quenching [K_{sv1}(app) = 10 M^{-1}] than the EHNA complex [K_{sv1}(app) = 5 M^{-1}; not shown]. However, no dynamic quenching of component 1 by iodide (K_{sv1} <1 M^{-1}) is apparent in the enzyme–inhibitor complexes. This implies increases in the extent of static quenching, probably due to local conformation changes. Quenching of component 1 by 25 mM trichloroethanol was slightly enhanced by purine riboside (50%) and inhibited by deoxycoformycin (25%) compared to EHNA (40%) and enzyme alone (30%). The additional quenching in the enzyme–purine riboside complex was due to a drop in the lifetime of component 1.

Figure 6 summarizes the acrylamide quenching data for component 3 in the enzyme–inhibitor complexes. While EHNA decreases the accessibility of adenosine deaminase to acrylamide, binding of purine riboside seems to have little overall effect. The dynamic quenching of component 3 (not shown) is not affected by ground-state analogue inhibitors (K_{sv3} = 2 M^{-1}). As noted above, the center of gravity of component 3 of the enzyme–purine riboside complex shifts down to 336 nm, indicating enhanced dynamic quenching of the polar environment 3B relative to environment 3A over the uncomplexed enzyme. For both iodide and trichloroethanol, the quenching of component 3 is similar in the purine riboside and EHNA complexes and somewhat less than in enzyme alone (not shown).

Discussion

Adenosine deaminase is an important enzyme because of its role in maintaining immune competence. It is also a well-known model for studying tight-binding enzyme inhibitors. The primary structure of the human enzyme has been reported (Wiginton et al., 1984; Daddona et al., 1984), but almost no other structural information is available for adenosine deaminase from any source. We have used fluorescence to probe gross structural features of the human enzyme. In this paper, we focused on the structural perturbations that occur upon binding of ground- and transition-state analogue inhibitors.

The photophysical properties of tryptophan residues in proteins are notoriously complicated. Single tryptophans in peptide hormones and proteins often exhibit multiexponential fluorescence decays (Beechem & Brand, 1985). A variety of processes can result in complex decays: ground-state heterogeneity, solvent reorientation around the excited indole ring, internal mobility during the excited-state lifetime, and excited-state electron- or proton-transfer reactions, to name a few. It is not yet known whether these complex decays represent discrete lifetimes or continuous lifetime distributions (Alcala et al., 1987a). In a few cases the interpretation of fluorescence decay data from proteins is straightforward. James et al. (1985) reported a monoexponential decay from the single buried tryptophan in ribonuclease T1 at pH 5.5. The biexponential decay observed at neutral pH was attributed to two distinguishable protein conformations (Chen et al., 1987). In a study of three homologous azurins, the single buried tryptophan in apoazurin Pae has a monoexponential decay and the single surface tryptophan in apoazurin Afe has a biexponential decay (Petrich et al., 1987). The anisotropy decays show that the Pae tryptophan is rigidly held in the protein interior whereas the exposed Afe tryptophan has substantial flexibility. The more complex fluorescence properties of the two tryptophans in apoazurin Ade were interpreted in light of the results for the single-tryptophan azurins. At the other extreme, Ludescher et al. (1985) resolved a three- or four-exponential decay for the single surface tryptophan in phos-

pholipase A2. Alcala et al. (1987b) have analyzed the fluorescence decay of phospholipase A2 assuming lifetime distributions. Both groups have argued that the mobile tryptophan residue may sample many conformational substates, resulting in a distribution of decay rates rather than a few discrete lifetimes.

The independent emissions from two tryptophan residues in proteins have been identified by combining time-resolved emission spectroscopy and solute quenching studies. Ross et al. (1981) observed a double-exponential decay for horse liver alcohol dehydrogenase. They were able to separate the spectra of the two lifetime components and assign the decays to a buried and an exposed tryptophan. The single-exponential decay of each tryptophan was explained by a rigid environment in the protein. Eftink et al. (1987) also reported that the individual tryptophans in several two-tryptophan-containing proteins appear to emit independently. Similar approaches have been taken to multitryptophan proteins, where the emission is described in terms of lifetime classes or distributions. Desie et al. (1986) resolved three temporally and spectrally distinct exponential decays in crystalline α-chymotrypsin. They used tryptophan–tryptophan energy-transfer efficiencies calculated from the X-ray coordinates as well as proximities of internal quenching groups to assign the eight tryptophans to the three lifetime classes. For low-density lipoproteins, Spragg and Wijnaendts van Resandt (1984) found that the environments of the 22 or more tryptophans were similar and concluded that the fluorescence decay was a continuous distribution of exponentials with a single maximum. Human adenosine deaminase has four tryptophans at positions 117, 161, 264, and 272 in a polypeptide chain of 362 amino acids (Daddona et al., 1984). The rotational correlation time of the enzyme may be estimated from the values of the steady-state anisotropy r and the mean lifetime $\langle\tau\rangle = \sum_i \alpha_i \tau_i^2 / \sum_i \alpha_i \tau_i$. Assuming a limiting anisotropy $r_0 = 0.17$–0.19 typical of tryptophan in proteins at 295-nm excitation wavelength (Lakowicz et al., 1983) and using $r = 0.12$ and $\langle\tau\rangle = 3.5$ ns at 340-nm emission wavelength, the apparent rotational correlation time is 6–8 ns. This value is lower than the about 16-ns rotational correlation time expected for a globular protein of molecular weight 41 000, suggesting that some or all of the tryptophans may be in mobile environments in the protein. Thus, a one-to-one correlation between individual tryptophan residues and the four tryptophan environments described in Table V is improbable. Nevertheless, partitioning the emission into decay-associated spectra and perturbing the component spectra with solute quenchers and inhibitors does provide qualitative information about the tryptophan environments in adenosine deaminase.

We have resolved the fluorescence decay of adenosine deaminase into three exponential components. Recovery of the decay parameters was aided by two factors: (1) global analysis, which reduces the number of degrees of freedom in the data analysis, and (2) reference deconvolution, which circumvents some experimental errors. The light scattering correction in the reference method is rigorous only for light scattered at the emission wavelength (Kolber & Barkley, 1986). This correction was essential for studying the short-lifetime component in PBS solutions. The scattering appears to be due to the formation of soluble aggregates of adenosine deaminase at low salt, since no scattering occurs at the same protein concentrations in high-salt solutions. After correction for scattered light, the lifetimes and decay-associated spectra of the three components are about the same at low and high salt in both the absence and presence (not shown) of inhibitors. This lends credence to the light scattering correction and argues against major salt-dependent changes in protein conformation. However, we cannot rule out the possibility of a subnanosecond decay in low-salt solutions of the enzyme, which masquerades as stray light. Given the potential complexity in a four-tryptophan protein, the three exponential decays only represent an empirical fit of the data. The underlying decay kinetics may include discrete lifetimes, multimodal lifetime distributions, or both. The emission spectra of the various tryptophan environments are partially separated in the decay-associated spectra. Components 1 and 2 have about the same emission maxima near 330 nm, though the centers of gravity are slightly different. Component 3 has an emission maximum at about 340 nm and comprises at least two overlapping spectra. We have claimed that inhibitor binding causes static quenching of adenosine deaminase fluorescence. Since we are unable to resolve the emissions of individual tryptophans, we cannot completely exclude dynamic quenching processes. If lifetime drops occurred, we should have seen emission transfer from a longer to a shorter lifetime class. This would increase the values of the preexponentials of short-lifetime components at the expense of long-lifetime components. Although we did not observe net increases in the preexponentials of components 1 and 2, small increases offset by larger decreases would have escaped detection.

Similar caveats apply to the solute quenching studies, where we typically found appreciable differences in the intensity and lifetime Stern–Volmer constants. Our interpretations of these results in terms of static and dynamic quenching are tentative. In the case of the enzyme–purine riboside complex, there was clear evidence of emission transfer from component 3 to component 1. Static quenching by acrylamide or trichloroethanol is a common phenomenon, though usually not at the low concentrations used in our experiments. Eftink and Ghiron (1987) showed that acrylamide does not bind significantly to proteins. To our knowledge, static quenching by iodide has not been reported. Since all three lifetime components are sensitive to low quencher concentrations and the trends in the acrylamide and iodide quenching data are parallel, it is entirely possible that we have underestimated the extent of dynamic quenching. Recently, Lakowicz et al. (1987) have called attention to transient effects in protein quenching experiments. They detected increased heterogeneity in the decay of the single tryptophan in staphylococcal nuclease in the presence of 0.19 M acrylamide due to a time-dependent rate constant for quenching. The decay of horse liver alcohol dehydrogenase also becomes more heterogeneous above 0.1 M iodide (Demmer et al., 1987). We found no evidence for additional decay components in adenosine deaminase in the presence of acrylamide or iodide. However, transient effects are manifest as extrashort-lifetime components, which would have been difficult to resolve in our case.

In principle, the Stern–Volmer constants extracted from time-resolved and steady-state quenching experiments can be compared. The apparent quenching parameters from steady-state studies of multitryptophan proteins are weighted functions of the dynamic and static quenching constants of the individual tryptophans (Lehrer & Leavis, 1978). At low concentrations of quencher the slope of a Stern–Volmer plot K_{sv} or the inverse slope of a modified Stern–Volmer plot $f_a K_{sv}$ is $K_{sv}(\text{eff}) = \sum f_i K_{svi}(\text{app})$, where f_i is the fractional intensity and $K_{svi}(\text{app})$ is the apparent quenching constant of tryptophan i. Although our lifetime components do not represent individual tryptophans in adenosine deaminase, we can still estimate $K_{sv}(\text{eff})$ from the $K_{svi}(\text{app})$ values for the intensity drops

of the decay-associated spectra and $f_i = \alpha_i\tau_i/\sum_i\alpha_i\tau_i$. For example, the K_{sv}(eff) values were 8.0 and 4.5 M^{-1} for acrylamide and iodide quenching of adenosine deaminase. These values can be compared to f_aK_{sv} values of 7.8 and 4.0 M^{-1} obtained from the modified Stern–Volmer plots of the steady-state data (Philips et al., 1986). The enzyme–EHNA complex gave K_{sv}(eff) values of 5.5 and 3.6 M^{-1} for acrylamide and iodide quenching, in rough agreement with the f_aK_{sv} values of 2.9 and 2.5 M^{-1}. Thus, the effective quenching constants estimated from the time-resolved data appear in reasonable accord with the steady-state values. The steady-state spectrum of adenosine deaminase shifts about 3 nm to the blue in the presence of 1 M acrylamide or iodide (Philips et al., 1986). Presumably, these spectral shifts reflect preferential quenching of component 3B.

The essential conclusions of the time-resolved fluorescence studies of adenosine deaminase are the following: (1) purine riboside and deoxycoformycin quench the emission of one tryptophan environment to different extents, and (2) ground- and transition-state analogue inhibitors have different effects on the accessibility of other tryptophan environments in the protein to solute quenchers. Because only one decay-associated spectrum is affected by both purine riboside and deoxycoformycin, it is tempting to speculate that component 2 represents a tryptophan environment near the active site of adenosine deaminase. The differential quenching of component 2 by the ground- and transition-state analogues could mean that progress from a ground-state to a transition-state complex involves a local structural rearrangement at the site. This could account for the biphasic kinetics of the fluorescence decrease which occurs upon binding of deoxycoformycin (Philips et al., 1986). EHNA, an adenosine analogue with a hydrophobic tail in place of the ribose moiety, may not bind directly at the site (Woo & Baker, 1982). Component 2 represents a nonpolar environment with an emission maximum around 330 nm. A hydrophobic active site is consistent with results for calf adenosine deaminase when a dansylated adenosine is used to probe the site (Skorka et al., 1981). Another interpretation is suggested by the recent finding that adenosine deaminase converts purine riboside into a tetrahedral form at C-6 in the enzyme–inhibitor complex (Kurz & Frieden, 1987). In this case both purine riboside and deoxycoformycin would form transition-state complexes. Because the heteroatom bound to the tetrahedral carbon is donated by the protein in the purine riboside complex and by the inhibitor in the deoxycoformycin complex, the fluorescence quenching of component 2 would undoubtedly be different.

Alternatively, the differential quenching of component 2 may reflect protein conformation changes remote from the active site upon binding of ground- and transition-state analogue inhibitors. The three inhibitors that we used all interact differently at the active site and induce different accessibility changes in components 1 and 3. The changes in accessibility probably reflect subtle conformational alterations in the protein, since they appear to involve changes in the degree of static quenching. A plausible explanation for a change in static quenching might be a change in the polarity of the tryptophan environments caused by reorientation of nearby side chains. Calf adenosine deaminase has been extensively studied by a variety of kinetic approaches. The binding of transition-state analogue inhibitors is characterized by an apparent slow rate constant as an initial step. This weak binding step appears to be followed by a conformation change in the protein and tighter binding of the inhibitor (Kurz & Frieden, 1983). Apparent second-order rate constants for transition-state analogue inhibitor binding have been further correlated with a viscosity-dependent change in the conformation of calf adenosine deaminase (Kurz et al., 1987).

The secondary structure of adenosine deaminase has been predicted by Daddona et al. (1984) from smoothed curves of amino acid conformational preference parameters (Palau et al., 1982). In this algorithm, the probability of an amino acid being in a particular secondary structure is calculated as the ratio of its occurrence in the secondary structure to that in the protein database of 44 known tertiary structures. Protein structure predictions are typically about 60% accurate. The predicted secondary structure of adenosine deaminase has a $\beta\alpha\beta$-like pattern within the 200 N-terminal residues, which may be a possible adenosine-binding pocket (Daddona et al., 1984). There are two tryptophans in this region (tryptophan-117 and tryptophan-161).

In conclusion, we have performed the first physical studies of human adenosine deaminase. The time-resolved fluorescence experiments reported in this paper have confirmed and extended our conclusions based on previous steady-state fluorescence results. Protein conformation changes occur upon binding of ground- and transition-state analogue inhibitors. More detailed analysis of these conformation changes will require the use of engineered adenosine deaminase proteins containing fewer tryptophans. This work is currently in progress.

ACKNOWLEDGMENTS

We thank John May for graphics and Dr. Jay R. Knutson for helpful discussions during preparation of the manuscript.

REFERENCES

Agarawal, R. P., Cha, S., Crabtree, G. W., & Parks, R. E., Jr. (1978) in *Symposium of Chemistry and Biology of Nucleosides and Nucleotides* (Robins, R. K., & Harmon, R. E., Eds.) ACS Advances in Chemistry Series, pp 159–197, Academic Press, New York.

Alcala, J. R., Gratton, E., & Prendergast, F. G. (1987a) *Biophys. J. 51*, 597–604.

Alcala, J. R., Gratton, E., & Prendergast, F. G. (1987b) *Biophys. J. 51*, 925–936.

Beechem, J. M., & Brand, L. (1985) *Annu. Rev. Biochem. 54*, 43–71.

Bevington, P. R. (1969) *Data Reduction and Error Analysis for the Physical Sciences*, McGraw-Hill, New York.

Chen, L. X.-Q., Longworth, J. W., & Fleming, G. R. (1987) *Biophys. J. 51*, 865–873.

Daddona, P. E., Shewach, D. S., Kelley, W. N., Argos, P., Markham, A. F., & Orkin, S. H. (1984) *J. Biol. Chem. 259*, 12101–12106.

Demmer, D. R., James, D. R., Steer, R. P., & Verrall, R. E. (1987) *Photochem. Photobiol. 45*, 39–48.

Desie, G., Boens, N., & DeSchryver, F. C. (1986) *Biochemistry 25*, 8301–8308.

Eftink, M. R., & Ghiron, C. A. (1981) *Anal. Biochem. 114*, 199–227.

Eftink, M. R., & Ghiron, C. A. (1987) *Biochim. Biophys. Acta 916*, 343–349.

Eftink, M. R., Zajicek, J. L., & Ghiron, C. A. (1977) *Biochim. Biophys. Acta 491*, 473–481.

Eftink, M. R., Wasylewski, Z., & Ghiron, C. A. (1987) *Biochemistry 26*, 8338–8346.

Evans, B., & Wolfenden, R. (1970) *J. Am. Chem. Soc. 92*, 4751–4752.

Freiden, C., Kurz, L. C., & Gilbert, H. R. (1980) *Biochemistry 19*, 5303–5309.

Giblett, E. R., Anderson, J. E., Cohen, F., Pollara, B., & Meuwissen, H. J. (1972) *Lancet 2*, 1067–1069.
Grinvald, A., & Steinberg, I. Z. (1974) *Anal. Biochem. 59*, 583–598.
James, D. R., Demmer, D. R., Steer, R. P., & Verrall, R. E. (1985) *Biochemistry 24*, 5517–5526.
Knutson, J. R., Beechem, J. M., & Brand, L. (1983) *Chem. Phys. Lett. 102*, 501–507.
Kolber, Z. S., & Barkley, M. D. (1986) *Anal. Biochem. 152*, 6–21.
Kurz, L. C., & Frieden, C. (1983) *Biochemistry 22*, 382–389.
Kurz, L. C., & Frieden, C. (1987) *Biochemistry 26*, 8450–8457.
Kurz, L. C., LaZard, D., & Frieden, C. (1985) *Biochemistry 24*, 1342–1346.
Kurz, L. C., Weitkamp, E., & Frieden, C. (1987) *Biochemistry 26*, 3027–3032.
Lakowicz, J. R. (1983) *Principles of Fluorescence Spectroscopy*, Plenum Press, New York.
Lakowicz, J. R., & Hogen, D. (1981) *Biochemistry 20*, 1366–1373.
Lakowicz, J. R., Maliwal, B. P., Cherek, H., & Balter, A. (1983) *Biochemistry 22*, 1741–1752.
Lakowicz, J. R., Joshi, N. B., Johnson, M. L., Szmacinski, H., & Gryczynski, I. (1987) *J. Biol. Chem. 262*, 10907–10910.
Lehrer, S. S., & Leavis, P. C. (1978) *Methods Enzymol. 49*, 222–236.
Lowry, O. H., Rosebrough, N. J., Farr, A. L., & Randall, R. J. (1951) *J. Biol. Chem. 193*, 265–275.
Ludescher, R. P., Volwerk, J. J., deHaas, G. H., & Hudson, B. S. (1985) *Biochemistry 24*, 7240–7249.
Palau, J., Argos, P., & Puigdomenech, P. (1982) *Int. J. Peptide Protein Res. 19*, 394–401.
Petrich, J. W., Longworth, J. W., & Fleming, G. R. (1987) *Biochemistry 26*, 2711–2722.
Philips, A. V., Robbins, D. R., Coleman, M. S., & Barkley, M. D. (1986) *Biochemistry 26*, 2893–2903.
Ross, J. B. A., Schmidt, C. J., & Brand, L. (1981) *Biochemistry 20*, 4369–4377.
Skorka, G., Shuker, P., Gill, D., Zabicky, J., & Parola, A. H. (1981) *Biochemistry 20*, 3103–3109.
Spragg, S. P., & Wijnaendts Van Resandt, R. W. (1984) *Biochim. Biophys. Acta 792*, 84–91.
Wiginton, D. A., Adrian, G. S., & Hutton, J. J. (1984) *Nucleic Acids Res. 12*, 2439–2445.
Woo, P. W. K., & Baker, D. C. (1982) *J. Med. Chem. 25*, 603–605.

^{31}P NMR of Covalent Phosphorylated Derivatives of α-Chymotrypsin†

David G. Gorenstein,*,‡ Dinesh Shah,§ Rouhlwai Chen,§ and Deborah Kallick§

Department of Chemistry, Purdue University, West Lafayette, Indiana 47907, and Department of Chemistry, University of Illinois at Chicago, Chicago, Illinois 60680

Received May 16, 1988; Revised Manuscript Received August 17, 1988

ABSTRACT: The structures of various covalent phosphorylated derivatives of α-chymotrypsin (α-CT) have been studied by ^{31}P NMR spectroscopy. Diisopropylphosphoryl-α-chymotrypsin (α-DIPCT) shows a single ^{31}P signal at ca. 0.0 ppm (pH 4). At low pH, the ^{31}P NMR spectrum of α-DIPCT gradually changed with the appearance of one or two additional peaks. The ratio of the peaks varied with pH, time, and concentration. One of these two new downfield peaks (both at ca. 2.0 ppm) has been previously identified by Markley and co-workers (Markley, 1979; Porubcan et al., 1979) and van der Drift et al. (1985) as an aged monoisopropylphosphoryl-α-chymotrypsin (α-MIPCT) and is confirmed by our studies. A new additional downfield signal, separate from the α-MIPCT signal, is attributed to a dimer of the phosphorylated α-DIPCT. Phosphorylation of the enzyme with diphenyl chlorophosphate yields a monophenylphosphoryl-α-chymotrypsin (α-MPPCT) that also showed a single ^{31}P signal at −2.1 ppm (pH 7). However, the spectrum did not change as a function of pH, incubation time, or concentration. Comparison of the ^{31}P chemical shifts of the native and denatured phosphorylated derivatives of α-chymotrypsin suggests changes in the conformation about the P–O ester bonds are at least partially responsible for the various ^{31}P chemical shift differences.

Many of the serine proteinases and serine esterases are irreversibly inhibited by phosphorylating agents such as diisopropyl fluorophosphate (DFP) (Hartley, 1960). This inhibition is a result of the covalent binding of the diisopropylphosphoryl (DP) group to the γ-oxygen of the active-site serine residue (Osterbaan et al., 1955; Schaffer et al., 1953, 1954). The phosphorylated enzyme forms a stable, tetrahedral adduct (Figure 1) that is considered to be a good transition-state analogue (Lienhard, 1973; Stroud et al., 1974; Wolfenden, 1972; Kossiakoff & Spencer, 1981).

The structure of these irreversibly inhibited phosphorylated derivatives has been studied by ^{31}P NMR (Gorenstein & Findlay, 1976; Kallick et al., 1983; Markley, 1979; Porubcan et al., 1979; Reeck et al., 1977; Shah et al., 1983; van der Drift et al., 1985). ^{31}P chemical shifts are sensitive to both bonding and nonbonding interactions with the environment as well as to subtle geometric alterations about the phosphate tetrahedron

† Supported by NIH (GM36281), NSF (BBS 8614177), the Purdue University Biochemical Magnetic Resonance Laboratory, which is supported by NIH (Grant RR01077 from the Biotechnology Resources Program of the division of Research Resources), and the NSF National Biological Facilities Center on Biomolecular NMR, Structure and Design at Purdue (Grant BBS 8714258 from the Division of Biological Instrumentation).

‡ Purdue University.
§ University of Illinois at Chicago.

0006-2960/89/0428-2050$01.50/0